



Cite this: *Mater. Adv.*, 2023, 4, 1935

## Surface engineering of $\text{CsPbBr}_3$ perovskite nanocrystals: hole transfer dynamics and enhanced photocurrent response using a novel organic molecule<sup>†</sup>

D. Venkateswarlu,<sup>‡ab</sup> T. Swetha,<sup>‡a</sup> Syed Akhil,<sup>‡ac</sup> Manoj Palabathuni,<sup>c</sup> Nimai Mishra  <sup>c</sup> and Surya Prakash Singh  <sup>ab</sup>

In the last few years, cesium lead bromide ( $\text{CsPbBr}_3$ ) perovskite nanocrystals (PNCs) have achieved tremendous recognition due to their state-of-the-art photophysical properties. A hybrid combination of perovskite nanocrystals with organic molecules could be a viable option for efficient charge separation at the interface. However, the surface chemistry of PNCs plays a pivotal role, which determines the excited state of these PNCs and interactions with charge shuttle redox-active molecules. Efforts are being made to find suitable organic molecules that can efficiently extract charges from these nanocrystals. But the choices of organic molecules are limited. Herein, we have reported a novel organic hole acceptor, *i.e.* fluorene derivative 7,7-diethyl-5,7-dihydroindeno[2,1-*b*]carbazole (SPS-Cbz), and investigated the effect of nanocrystal surface chemistries for surface-bound charge transfer. We evaluated the photoinduced hole transfer (PHT) using the time-resolved PL lifetime decay curves and steady-state PL. We interestingly found that amine-free  $\text{CsPbBr}_3$  PNCs have five times higher PHT compared with conventional amine-based  $\text{CsPbBr}_3$  PNCs. The hole transfer rate constant ( $K_{ht}$ ) is  $6.96 \times 10^8 \text{ S}^{-1}$ , calculated using lifetime fast component rate constants ( $\tau_1$ ) from the lifetime decay curves, which is three times higher than that of amine-based ligand  $\text{CsPbBr}_3$  PNCs. Furthermore, photocurrent density studies were carried out and it was found that amine-free nanocrystals with SPS-Cbz were two times higher than bare amine-free  $\text{CsPbBr}_3$  PNCs. This work envisioned a judicious selection of organic acceptors that can make an efficient hybrid combination with perovskite nanocrystals for efficient charge separation, which implies various photonic applications.

Received 18th January 2023,  
Accepted 21st March 2023

DOI: 10.1039/d3ma00035d

[rsc.li/materials-advances](http://rsc.li/materials-advances)

## Introduction

The worldwide reliance on optoelectronic devices is rising and it is essential to produce more efficient optoelectronic materials with economical cost and faster production.<sup>1</sup> Recently, colloidal semiconductor metal halide perovskite nanocrystals (PNCs) have gotten special recognition across the materials research community.<sup>2</sup> In particular, all-inorganic cesium lead halide  $\text{CsPbX}_3$  (X = Cl, Br, and I) PNCs are one of the emerging photonic

materials due to their novel optoelectronic properties.<sup>3</sup> These materials have broad absorbance,<sup>4</sup> narrow emissions with wide spectral tunability in the entire visible region by halide exchange,<sup>5</sup> reduced photoluminescence (PL) blinking,<sup>6</sup> low exciton binding energy, long diffusion length, and near-unity photoluminescence quantum yield (PLQY).<sup>5</sup> All the aforesaid outstanding optoelectronic properties make this material an ideal candidate for solar cells,<sup>7</sup> lasers,<sup>8</sup> light-emitting diodes (LEDs),<sup>9</sup> sensors,<sup>10</sup> scintillators,<sup>11</sup> and photodetectors.<sup>12</sup> Studies show that PNCs undergo fast electron/hole transfer with photoredox molecules.<sup>13,14</sup>  $\text{CsPbBr}_3$  PNCs are the most studied and robust among other inorganic PNCs, having narrow and bright green emissions with less than 25 nm of full-width at half maximum (FWHM)<sup>15</sup> and showing potential in various applications.<sup>16</sup>

In  $\text{CsPbX}_3$  PNCs, the carrier diffusion plays a vital role in optoelectronic devices; these depend on various elements such as exciton binding energy, conduction and valence bands (energy levels), surface chemistry, and crystallinity of the PNCs.<sup>14,17,18</sup> Upon photoexcitation in the optoelectronic devices, the exciton

<sup>a</sup> Polymers and Functional Materials Division, CSIR-Indian Institute of Chemical Technology, Uppal Road, Tarnaka, Hyderabad-500007, India.

E-mail: [spsingh@iict.res.in](mailto:spsingh@iict.res.in)

<sup>b</sup> Academy of Scientific and Innovative Research (AcSIR), Ghaziabad, Uttar Pradesh 201002, India

<sup>c</sup> Department of Chemistry, SRM University-AP, Neerukonda, Mangalagiri, Guntur-522240, Andhra Pradesh, India

† Electronic supplementary information (ESI) available. See DOI: <https://doi.org/10.1039/d3ma00035d>

‡ These authors contributed equally.



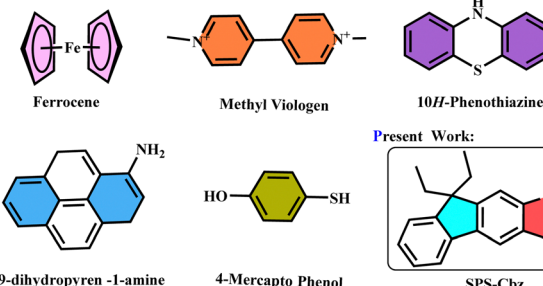
dissociates into hole/electron donors and is transferred to the hole/electron acceptor molecules of the valence/conduction bands, respectively. However, these perovskite nanocrystals have been used as visible light photoredox catalysts for organic synthesis with limited substrate scope.<sup>19</sup> The reason behind this limitation is due to the high energy barrier surfactants on the surface of these PNCs, and material instability in the polar solvents. However, surfactants are unavoidable during the synthesis and restrict access to hole/electron acceptors on the active surface sites of PNCs.

Surface engineering is essential to fine tune the perovskite photophysical and electrochemical properties for its various applications, such as the position of the conduction and valence band edge energies.<sup>20</sup> The incorporation of surface ligands helps in improving the solubility and excited-state interaction in such types of hybrid structures.<sup>21</sup> Recently, a library of surfactants has been explored to stabilize the PNCs by using alkyl phosphine ligands,<sup>22,23</sup> zwitterion ligands,<sup>24</sup> and quaternary amines.<sup>25</sup> These surface ligands stabilize the PNCs from external environments like moisture, light irradiation *etc.*<sup>3</sup> Thus, choosing the ligands has been quite challenging; the ligand branching<sup>26</sup> and the amounts of ligand<sup>27</sup> impact the dimensionality of PNCs and in some cases, their stoichiometry may lead to the formation of  $\text{CsPbBr}_5$  and  $\text{Cs}_4\text{PbBr}_6$ .<sup>29</sup>

Recently,  $\text{CsPbBr}_3$  PNCs have been explored as photocatalysts. Lian's group studied the charge carrier dynamics between benzooquinone (BQ) electron acceptor and phenothiazine (PTZ) as hole acceptor molecules with  $\text{CsPbBr}_3$  PNCs.<sup>13</sup> Later, Mandal *et al.* studied the electron and hole transfer processes followed by recombination dynamics of photoexcited charge carriers in perovskite PNC-molecular acceptor complexes.<sup>30</sup> Furthermore, Bose *et al.* examined the consequence of different surface chemistries based on  $\text{CsPbBr}_3$  PNCs on the photoredox methyl viologen molecules for their excited-state interactions and charge transfer studies.<sup>14</sup> Recently, the redox activities of the three various surface chemistries based on  $\text{CsPbBr}_3$  PNCs were investigated to study the photoinduced hole and electron transfer with PTZ hole and BQ electron acceptors. So far, commercially available hole acceptors like phenothiazine, 2-amino pyridine, thiophene, amino pyrene, ferrocene, and 4-mercaptoproethanol have been explored.<sup>31–34</sup> However, dynamic study on  $\text{CsPbBr}_3$  PNC-based hole transfer is not explored much; therefore, the development of new hole acceptor organic molecules to study their photoexcited hole transfer and furthermore understanding of the impact on hole transfer rates based on the different surfactants on the PNCs is important. Thus, there is a scope to improve the hole transfer efficiency by introducing novel organic molecules.

In search of suitable composites, there is a need for a good and efficient hole acceptor, which could improve the interaction with the  $\text{CsPbBr}_3$  PNC surface and at the same time act as an efficient hole acceptor. Herein, we have employed an efficient hole acceptor with better charge transport properties to get insight into the surface ligand-dependent charge transfer. Compared to the earlier reported organic hole-acceptors, SPS-Cbz contains poly-hetero aromatic rings, which leads to specific stability from its resonance delocalization of  $\pi$ -electrons, and

Previously reported hole-transfer molecules



Present Work:

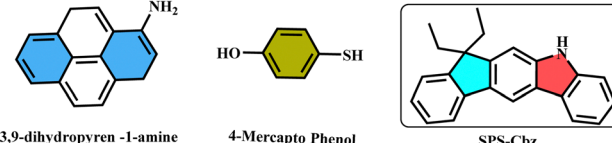


Fig. 1 (a) Previously reported hole transfer molecules and (b) newly synthesized hole transfer molecule SPS-Cbz.

the non-fluorescent nature of this molecule makes it a good quencher (Fig. 1).

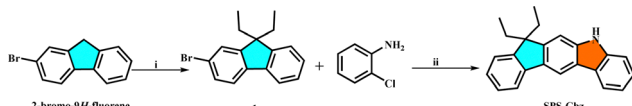
We have synthesized two different  $\text{CsPbBr}_3$  PNCs, namely amine-free  $\text{CsPbBr}_3$  PNCs, where oleic acid (OA) and trioctylphosphine (TOP) are used as surfactants, and amine-based  $\text{CsPbBr}_3$  PNCs, where OA and oleylamine (OAm) are used as surfactants. The synthesized PNCs were used as photoinduced-hole donors and a newly synthesized organic molecule, fluorene (SPS-Cbz), as the hole acceptor to understand the surfactant-dependent charge (hole) transfer from PNCs to the hole acceptor and examine the photoinduced hole transfer (PHT). Using time-resolved PL (TRPL) and steady-state PL spectroscopy, we have studied the PHT process of  $\text{CsPbBr}_3$  PNCs, after addition of different concentrations of SPS-Cbz.

Interestingly, from steady-state PL, we found that amine-free  $\text{CsPbBr}_3$  PNCs show enhanced photoinduced hole transfer compared with amine-based PNCs. Due to the absence of strong binding nature of OAm, amine-free PNCs facilitate faster hole transfer. Furthermore, it was confirmed by TRPL, where amine-free PNCs have long lifetime, indicating the longer existence of the exciton, which can readily dissociate and transfer to the SPS-Cbz-hole acceptor molecule. We have calculated the Stern–Volmer constant ( $K_{\text{SV}}$ ) using the steady state PL. Also from  $K_{\text{SV}}$  and TRPL we estimated the bi-molecular quenching constant ( $K_{\text{q}}$ ). In addition, we have investigated the hole transfer rate constant ( $K_{\text{ht}}$ ) from the TRPL lifetime's fast component parameter. In the case of amine-free PNCs, the PHT process is five times higher than the amine-based one, with three times higher hole transfer rate constant ( $K_{\text{ht}}$ ). Therefore, here we envisioned that utilization of novel organic molecule SPS-Cbz with the combination of amine-free  $\text{CsPbBr}_3$  PNCs may give a new direction for various applications. Previously reported and newly synthesized SPS-Cbz molecules are presented in Fig. 1.

## Results and discussions

The complete synthetic pathways for SPS-Cbz are mentioned in Scheme 1 and a detailed synthetic procedure is provided in the ESI.† **1** is synthesized by alkylation of commercially available 2-bromo 9H fluorene followed by cyclization of **1** with 2-chloro aniline to achieve our target molecule SPS-Cbz in an 80% yield.  $\text{CsPbBr}_3$  PNCs were synthesized using the hot-injection method following previously reported protocols.<sup>35</sup> Moreover, synthesis of





**Scheme 1** Reagents and conditions: (i) KOH, 2-bromo ethane, DMSO, and 24 h, (ii)  $\text{Pd}_2(\text{dba})_3$ ,  $\text{PPh}_3$ ,  $\text{K}^t\text{OBu}$ , toluene, and 48 h, yield = 80%.

PNCs, DFT study of SPS-Cbz, and  $^1\text{H}/^{13}\text{C}$  NMR and mass analysis are presented in the ESI<sup>†</sup> (Fig. S1–S7 and Tables S1 and S2, ESI<sup>†</sup>).

We have studied the absorption spectra of SPS-Cbz in dichloromethane solvent (Fig. 2a) ranging from 250 nm to 600 nm. The absorption maximum ( $\lambda_{\text{max}}$ ) was found to be at 335 nm, which was attributed to intramolecular charge transfer (ICT) and the  $\pi-\pi^*$  transitions were observed at 265 nm. The PL spectra were recorded at the excitation wavelength of 335 nm and the characteristic vibronic emission band was observed at 360 nm. To determine the energy levels (highest occupied molecular orbital (HOMO) and lowest unoccupied molecular orbital (LUMO)) of SPS-Cbz we have performed cyclic voltammetric measurements using a three-electrode system (Fig. 2b). The HOMO is located at  $-5.59$  eV and the LUMO is at  $-2.10$  eV. Based on the redox properties of the newly synthesized hole acceptor molecule, it facilitates enough driving force for hole transfer from  $\text{CsPbBr}_3$  PNCs to the SPS-Cbz molecule.

The complete characterizations of both the amine-free and amine-based PNCs are shown in Fig. 3. The broad absorbance and narrow PL spectra of the two different surface system-based  $\text{CsPbBr}_3$  PNCs are demonstrated in Fig. 3(a). In the case of the amine-free system (blue lines), an absorption band ( $\lambda_{\text{max}}$ ) located at 515 nm, a PL peak at 519 nm with FWHM at 19.65 nm and PLQY of 0.80 were observed. Whereas, in the case of the amine-based system (black lines), an absorption peak ( $\lambda_{\text{max}}$ ) at 510 nm, PL peak at 513 nm with FWHM 23.45 nm and PLQY of 0.85 were observed. The XRD patterns of both the amine-free and amine PNCs are shown in Fig. 3(b), which resembles the previously reported data and confirms the orthorhombic phase.<sup>35</sup> Transmission electron microscopy images of amine-free and amine based- $\text{CsPbBr}_3$  PNCs are shown in Fig. 3(c and d), which reveal that the high-monodispersity particles are cubic in shape with average particle sizes of  $27.45 \pm 0.9$  nm and  $14.13 \pm 1.2$  nm, respectively. Because of the absence of the oleylamine quickening growth of PNCs, an increment in particle size happens in the amine-free PNCs compared to the amine-based PNCs.<sup>36</sup>

Due to their large molar extinction coefficients ( $\sim 10^6 \text{ M}^{-1} \text{ cm}^{-1}$ ) in the visible range of the  $\text{CsPbX}_3$  PNCs they exhibit excellent light

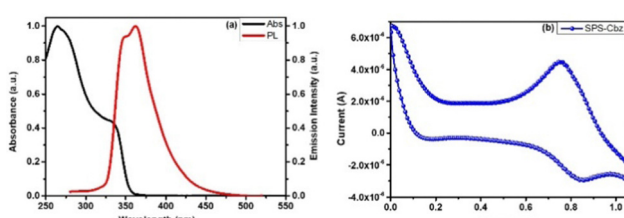


**Fig. 2** (a) UV-Vis absorbance and PL spectra. (b) Cyclic voltammogram of SPS-Cbz in DCM solvent.

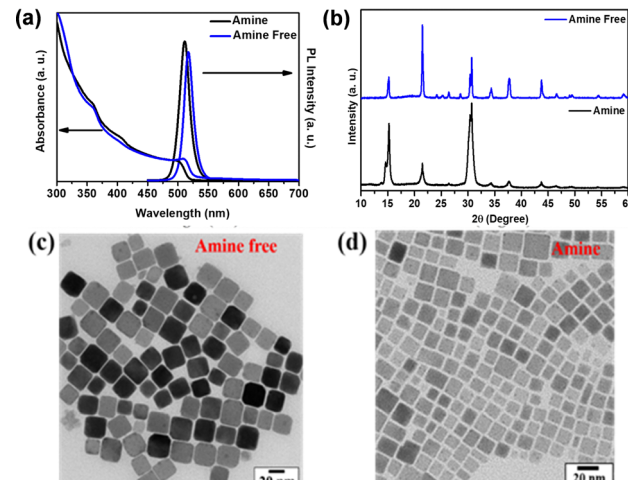


**Fig. 3** (a) UV-Vis absorbance and PL spectra. (b) X-ray diffraction spectra. (c and d) TEM images of the amine-free and amine-based PNCs, respectively.

absorption. Because of their low exciton binding energies, these PNCs exhibit successive photoinduced charge separation.<sup>13</sup> The surfactants play a crucial role in stabilizing the PNCs, but long-chain containing surfactants affect charge transfer from the PNCs to the charge acceptor molecules. As they are ionic in nature, these materials often suffer from dissolution/phase transformations.<sup>3</sup> Therefore, we have developed a simple and controllable method through molecularly engineered molecules and used a surface modulating ligand to overcome the stability issues.<sup>23,35</sup>

To begin, we have measured the absorption spectra of  $\text{CsPbBr}_3$  PNCs by sequential addition of SPS-Cbz for both the systems (*i.e.* amine-free and amine-based) in toluene (Fig. 4).<sup>37</sup>

As shown in Fig. 4(a and b) there are no apparent changes in the onset of the absorption band observed upon addition of SPS-Cbz in both the systems.

Next, we carried out the PL study of amine-free and amine- $\text{CsPbBr}_3$  PNCs after the progressive addition of SPS-Cbz molecules (0–0.6 mM) (Fig. 5a and b). The PL intensity was quenched on addition of the SPS-Cbz ligand. The digital images under UV light irradiation are displayed in Fig. 5. The fluorescence quenching data were analysed using eqn (1).

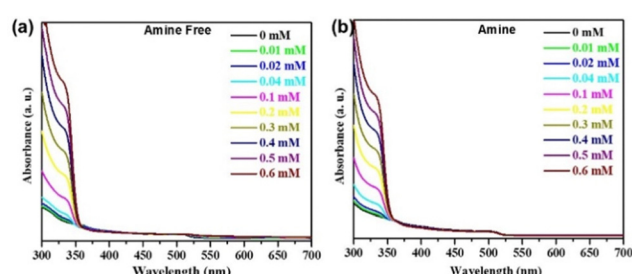


**Fig. 4** UV-Vis absorbance spectra of (a) amine-free and (b) amine-based PNCs with SPS-Cbz.



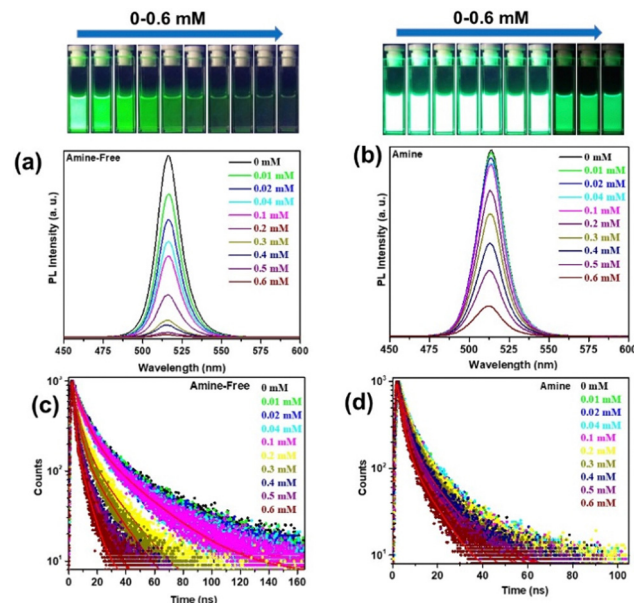


Fig. 5 (a and b) PL spectra and (c and d) TCSPC spectra of amine-free and amine-based PNCs with different concentrations of SPS-Cbz molecules.

The apparent association constant ( $K_{app}$ ) was also evaluated by using the double reciprocal plot of fluorescence quenching data between the  $\text{CsPbBr}_3$  PNCs and SPS-Cbz molecules following eqn (1). The binding interactions between the PNCs and SPS-Cbz are studied from the Benesi–Hildebrand equation by using the double reciprocal plot.<sup>38</sup> The  $K_{app}$  was calculated by  $1/(F_x - F_0) \text{ vs. } 1/[\text{SPS-Cbz}]$ , where  $F_x$  is PNCs PL intensity without the SPS-Cbz molecule, whereas  $F_0$  is the PNCs PL intensity upon addition of the quencher molecule at different concentrations (ESI,† Fig. S8). The  $K_{app}$  values are observed in similar order  $0.168 \times 10^3 \text{ M}^{-1}$  and  $0.852 \times 10^3 \text{ M}^{-1}$  for amine-free and amine-based PNCs, respectively. These results revealed that the binding between PNCs and SPS-Cbz are similar in both the systems though these PNCs have long chain surface capping ligands; still their surface easily interacts with the redox-active molecule.

Time-correlated single-photon counting (TCSPC) has been studied to determine the effect of SPS-Cbz on the excited states of  $\text{CsPbBr}_3$  PNCs (Fig. 5c and d). Amine-free  $\text{CsPbBr}_3$  PNCs have the highest lifetime of ( $\bar{\tau}_{avg} \sim 23.2 \text{ ns}$ ) compared to amine-based PNCs. After the addition of the SPS-Cbz molecule, the lifetime decreases drastically, which is attributed to hole transfer from the PNCs to surface-bound SPS-Cbz molecules.

From both the PL spectra and TRPL life time data it is clearly seen that there is significant quenching in PL intensity and a drastic decrease in life time decay in the case of the amine-free system, which indicates the faster photoinduced hole transfer process compared with amine-based PNCs. The photoinduced hole transfer process from PNCs to the SPS-Cbz is attributed in eqn (2).

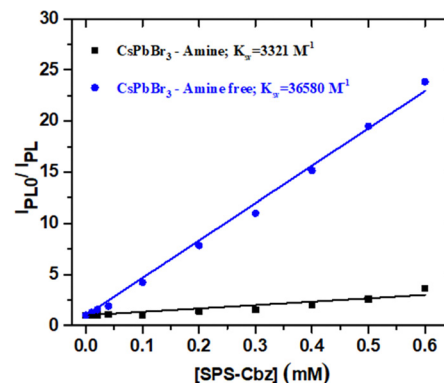
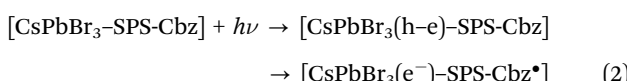


Fig. 6 The Stern–Volmer plots of amine-free (blue) and amine-based (black) PNCs with SPS-Cbz.

Moreover, we have quantitatively evaluated the PHT process using the steady-state PL and time-resolved photoluminescence (TRPL) of both the  $\text{CsPbBr}_3$  PNCs with addition of SPS-Cbz. The reduction potential of the PNCs and the surfactant permeability play a vital role in the PHT process.<sup>39</sup> Due to the dynamic quenching by the hole acceptor molecules, the PL and TRPL spectral intensities decrease significantly in the amine-free PNCs compared to the amine-based system.

The Stern–Volmer plots are presented in Fig. 6. Following eqn (3), we have studied the photoinduced charge transfer process.

$$I_{PL0}/I_{PL} = 1 + K_{SV}[\text{SPS-Cbz}] = 1 + K_q \bar{\tau}_0[\text{SPS-Cbz}] \quad (3)$$

Here,  $I_{PL0}$  and  $I_{PL}$  are the PL intensities without SPS-Cbz and with different concentrations of SPS-Cbz, respectively, and  $K_{SV}$  is the Stern–Volmer quenching constant of the steady state PL. In addition, the linear relationship between the  $I_{PL0}/I_{PL}$  vs. [SPS-Cbz] implies that the PHT process is diffusion-limited.<sup>40</sup>

From the Stern–Volmer quenching constant ( $K_{SV}$ ) and the average lifetime ( $\bar{\tau}_0$ ), bi-exponential fit of only bare  $\text{CsPbBr}_3$  PNCs, we can calculate the bimolecular quenching constant ( $K_q$ ). The amine-free system shows the highest  $K_{SV}$  compared to the amine-based  $\text{CsPbBr}_3$  PNCs. Moreover, the bimolecular quenching constant  $K_q$  was found to be 4.6 times higher compared with the amine-based  $\text{CsPbBr}_3$  PNCs. The detailed amine-free and amine-based  $\text{CsPbBr}_3$  PNC quenching data ( $K_{SV}$  and  $K_q$ ) and average lifetime constant ( $\bar{\tau}_0$ ) are tabulated in Table 1. As the amine-free PNCs show good surfactant permeability, they enhanced the redox potential properties.

Additionally, we have calculated the PLQY of both the PNCs at each sequential addition of SPS-Cbz molecules and the PLQY significantly decreases in amine-free compared with amine- $\text{CsPbBr}_3$  PNCs. Based on the PLQY and lifetime ( $\bar{\tau}_{avg}$ ) values, we have calculated the radiative ( $K_r$ ) and non-radiative ( $K_{nr}$ ) rate

Table 1 Photoinduced hole transfer parameters

$\text{CsPbBr}_3$ PNCs	$K_{SV} (\text{mM}^{-1})$	$\bar{\tau}_0 (\text{ns})$	$K_q (\text{M}^{-1} \text{ ns}^{-1})$	$K_q$ improvement
Amine-free	36.58	23.20	1576.72	4.65
Amine	3.32	9.76	340.27	1



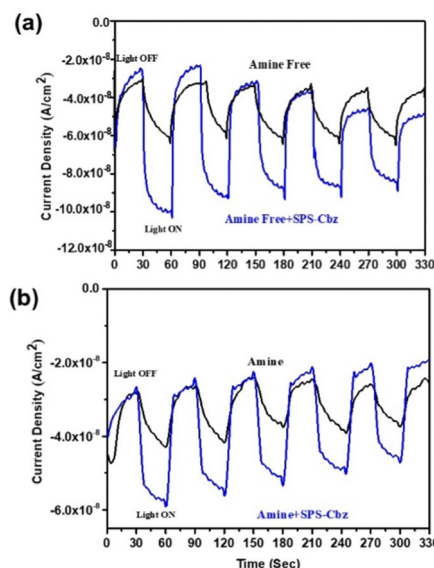


Fig. 7  $i$ – $t$  curves of (a) amine-free (black) and amine-free + SPS-Cbz (blue), and (b) amine (black) and amine + SPS-Cbz (blue)  $\text{CsPbBr}_3$  PNCs under AM 1G light illuminator ( $100 \text{ mW cm}^{-2}$ ).

constants where  $K_r$  is  $\text{PLQY}/\tau_{\text{avg}}$  and  $K_{\text{nr}}$  is  $(1-\text{PLQY})/\tau_{\text{avg}}$ . The detailed parameters such as the lifetime decay, PLQY, and radiative and non-radiative rate constants at each sequential addition of hole acceptor molecules for both the systems are presented in Tables S3 and S4 (ESI<sup>†</sup>).

Based on eqn (4), we have calculated the hole transfer rate constants ( $K_{\text{ht}}$ ), using fast time components ( $\tau_1$ ) of PNCs with and without SPS-Cbz.<sup>17</sup> After the analysis, we evaluated the  $K_{\text{ht}}$  values of  $6.96 \times 10^8$  and  $2.5 \times 10^8 \text{ s}^{-1}$  for amine-free and amine-based PNCs, respectively. We have concluded that the  $K_{\text{ht}}$  value is  $\sim 3$  times higher for amine-free than for the amine-based PNCs (Table S5, ESI<sup>†</sup>). Therefore, we presumed that our study on the hole transfer based on two surface engineered systems plays a crucial role in determining the charge separation/charge transfer processes.

$$k_{\text{ht}} = \frac{1}{\tau_1 \text{CsPbBr}_3 + \text{SPS-Cbz}(0.6 \text{ mM})} - \frac{1}{\tau_1 \text{CsPbBr}_3 + \text{SPS-Cbz}(0 \text{ mM})} \quad (4)$$

As a proof of concept, we have studied the photocurrent response of these PNCs (with and without SPS-Cbz, Fig. 7). The photocurrent  $\text{vs}$  time test was performed, and their photocurrents are reproducible upon the light source ON/OFF cycling. In amine-free + SPS-Cbz molecule, the photocurrent density is two folds higher than that of the bare amine-free  $\text{CsPbBr}_3$  PNCs (Fig. 7a). At the same time, amine-based PNCs + SPS-Cbz is 1.5 times higher than the bare amine (Fig. 7b). The photocurrent density followed the same trends as the photo-induced hole transfer processes. This indicates that the efficient charge transfer in the amine-free + SPS-Cbz is consistent with their PL, TRPL,  $K_{\text{SV}}$ , and  $K_{\text{q}}$  quenching constants.

## Conclusions

In summary, we have newly designed and synthesized a molecularly engineered small molecule SPS-Cbz and used it as a hole acceptor to study the photoinduced hole-transfer phenomenon. We have carried out the hole transfer studies with quantitatively photoinduced hole transfer processes for two different PNCs: amine-free (TOP/OA) and amine-based (OA/OAm). We interestingly found that in the amine-free system, the PHT process was five-times higher and the hole transfer rate constant ( $K_{\text{ht}}$ ) is three times higher than in the amine-based PNCs. The amine-free PNCs show two times higher photocurrent density compared to the amine-based PNCs. Therefore, it is crucial to understand the surface chemistry of PNCs for the surface state-mediated interfacial hole transfer rate. Finally, these studies provide insights for designing efficient halide perovskite nanocrystals and hole acceptor molecules.

## Author contributions

D.V. synthesized the SPS-Cbz molecule, T.S. carried out the characterizations and prepared the manuscript draft, and S.A. and P. M synthesized the PNCs and studied the charge transfer. N.M. supervised the charge transfer studies and S.P.S. designed the project, was responsible for overall supervision, and prepared the final manuscript.

## Conflicts of interest

There are no conflicts to declare.

## Acknowledgements

S.P.S acknowledges financial support from the Government of India, Department of Atomic Energy, BRNS (Sanction No. 58/14/01/2021-BRNS/37065). We thank the HRTEM FACILITY at SRMIST set up with support from MNRE (Project No. 31/03/2014-15/PVSR&D), the Government of India, CSIR-IICT Communication Number: IICT/Pubs./2022/380.

## Notes and references

- Q. A. Akkerman, G. Rainò, M. V. Kovalenko and L. Manna, *Nat. Mater.*, 2018, **17**, 394–405.
- A. Dey, J. Ye, A. De, E. Debroye, S. K. Ha, E. Bladt, A. S. Kshirsagar, Z. Wang, J. Yin, Y. Wang, L. N. Quan, F. Yan, M. Gao, X. Li, J. Shamsi, T. Debnath, M. Cao, M. A. Scheel, S. Kumar, J. A. Steele, M. Gerhard, L. Chouhan, K. Xu, X. Wu, Y. Li, Y. Zhang, A. Dutta, C. Han, I. Vincon, A. L. Rogach, A. Nag, A. Samanta, B. A. Korgel, C.-J. Shih, D. R. Gamelin, D. H. Son, H. Zeng, H. Zhong, H. Sun, H. V. Demir, I. G. Scheblykin, I. Mora-Seró, J. K. Stolarczyk, J. Z. Zhang, J. Feldmann, J. Hofkens, J. M. Luther, J. Pérez-Prieto, L. Li, L. Manna, M. I. Bodnarchuk, M. V. Kovalenko, M. B. J. Roeffaers, N. Pradhan, O. F. Mohammed, O. M. Bakr, P. Yang, P. Müller-Buschbaum, P. V. Kamat, Q. Bao,



Q. Zhang, R. Krahne, R. E. Galian, S. D. Stranks, S. Bals, V. Biju, W. A. Tisdale, Y. Yan, R. L. Z. Hoye and L. Polavarapu, *ACS Nano*, 2021, **15**, 10775–10981.

3 J. Shamsi, A. S. Urban, M. Imran, L. De Trizio and L. Manna, *Chem. Rev.*, 2019, **119**, 3296–3348.

4 V. G. V. Dutt, S. Akhil and N. Mishra, *ChemNanoMat*, 2020, **6**, 1730–1742.

5 L. Protesescu, S. Yakunin, M. I. Bodnarchuk, F. Krieg, R. Caputo, C. H. Hendon, R. X. Yang, A. Walsh and M. V. Kovalenko, *Nano Lett.*, 2015, **15**, 3692–3696.

6 A. Swarnkar, R. Chulliyil, V. K. Ravi, M. Irfanullah, A. Chowdhury and A. Nag, *Angew. Chem.*, 2015, **127**, 15644–15648.

7 A. Swarnkar, A. R. Marshall, E. M. Sanehira, B. D. Chernomordik, D. T. Moore, J. A. Christians, T. Chakrabarti and J. M. Luther, *Science*, 2016, **354**, 92–95.

8 J. Guo, T. Liu, M. Li, C. Liang, K. Wang, G. Hong, Y. Tang, G. Long, S.-F. Yu, T.-W. Lee, W. Huang and G. Xing, *Nat. Commun.*, 2020, **11**, 3361.

9 W. Xu, Q. Hu, S. Bai, C. Bao, Y. Miao, Z. Yuan, T. Borzda, A. J. Barker, E. Tyukalova, Z. Hu, M. Kawecki, H. Wang, Z. Yan, X. Liu, X. Shi, K. Uvdal, M. Fahlman, W. Zhang, M. Duchamp, J.-M. Liu, A. Petrozza, J. Wang, L.-M. Liu, W. Huang and F. Gao, *Nat. Photonics*, 2019, **13**, 418–424.

10 L. Gu, M. M. Tavakoli, D. Zhang, Q. Zhang, A. Waleed, Y. Xiao, K.-H. Tsui, Y. Lin, L. Liao, J. Wang and Z. Fan, *Adv. Mater.*, 2016, **28**, 9713–9721.

11 Q. Chen, J. Wu, X. Ou, B. Huang, J. Almutlaq, A. A. Zhumekenov, X. Guan, S. Han, L. Liang, Z. Yi, J. Li, X. Xie, Y. Wang, Y. Li, D. Fan, D. B. L. Teh, A. H. All, O. F. Mohammed, O. M. Bakr, T. Wu, M. Bettinelli, H. Yang, W. Huang and X. Liu, *Nature*, 2018, **561**, 88–93.

12 H. Wang and D. H. Kim, *Chem. Soc. Rev.*, 2017, **46**, 5204–5236.

13 K. Wu, G. Liang, Q. Shang, Y. Ren, D. Kong and T. Lian, *J. Am. Chem. Soc.*, 2015, **137**, 12792–12795.

14 J. T. DuBose and P. V. Kamat, *J. Phys. Chem. C*, 2020, **124**, 12990–12998.

15 X. Zhang, H. Lin, H. Huang, C. Reckmeier, Y. Zhang, W. C. H. Choy and A. L. Rogach, *Nano Lett.*, 2016, **16**, 1415–1420.

16 X. Zhu, Y. Lin, J. San Martin, Y. Sun, D. Zhu and Y. Yan, *Nat. Commun.*, 2019, **10**, 2843.

17 A. Giampietri, G. Drera and L. Sangaletti, *Adv. Mater. Interfaces*, 2017, **4**, 1700144.

18 C. de Weerd, L. Gomez, H. Zhang, W. J. Buma, G. Nedelcu, M. V. Kovalenko and T. Gregorkiewicz, *J. Phys. Chem. C*, 2016, **120**, 13310–13315.

19 V. Murugesh and S. P. Singh, *Chem. Rec.*, 2020, **20**, 1181–1197.

20 D. M. Kroupa, M. Vörös, N. P. Brawand, B. W. McNichols, E. M. Miller, J. Gu, A. J. Nozik, A. Sellinger, G. Galli and M. C. Beard, *Nat. Commun.*, 2017, **8**, 15257.

21 S. N. Raja, Y. Bekenstein, M. A. Koc, S. Fischer, D. Zhang, L. Lin, R. O. Ritchie, P. Yang and A. P. Alivisatos, *ACS Appl. Mater. Interfaces*, 2016, **8**, 35523–35533.

22 Y. Tan, Y. Zou, L. Wu, Q. Huang, D. Yang, M. Chen, M. Ban, C. Wu, T. Wu, S. Bai, T. Song, Q. Zhang and B. Sun, *ACS Appl. Mater. Interfaces*, 2018, **10**, 3784–3792.

23 S. Akhil, V. G. V. Dutt and N. Mishra, *Chem. – Eur. J.*, 2020, **26**, 17195–17202.

24 F. Krieg, S. T. Ochsenbein, S. Yakunin, S. ten Brinck, P. Aellen, A. Süess, B. Clerc, D. Guggisberg, O. Nazarenko, Y. Shynkarenko, S. Kumar, C.-J. Shih, I. Infante and M. V. Kovalenko, *ACS Energy Lett.*, 2018, **3**, 641–646.

25 Y. Shynkarenko, M. I. Bodnarchuk, C. Bernasconi, Y. Berezovska, V. Verteletskyi, S. T. Ochsenbein and M. V. Kovalenko, *ACS Energy Lett.*, 2019, **4**, 2703–2711.

26 J. Cho, Y.-H. Choi, T. E. O'Loughlin, L. De Jesus and S. Banerjee, *Chem. Mater.*, 2016, **28**, 6909–6916.

27 J. Cho, H. Jin, D. G. Sellers, D. F. Watson, D. H. Son and S. Banerjee, *J. Mater. Chem. C*, 2017, **5**, 8810–8818.

28 S. K. Balakrishnan and P. V. Kamat, *Chem. Mater.*, 2018, **30**, 74–78.

29 Z. Liu, Y. Bekenstein, X. Ye, S. C. Nguyen, J. Swabeck, D. Zhang, S.-T. Lee, P. Yang, W. Ma and A. P. Alivisatos, *J. Am. Chem. Soc.*, 2017, **139**, 5309–5312.

30 S. Sarkar, V. K. Ravi, S. Banerjee, G. R. Yettappu, G. B. Markad, A. Nag and P. Mandal, *Nano Lett.*, 2017, **17**, 5402–5407.

31 A. De, N. Mondal and A. Samanta, *J. Phys. Chem. C*, 2018, **122**, 13617–13623.

32 K. Chen, X. Deng, G. Dodekatos and H. Tüysüz, *J. Am. Chem. Soc.*, 2017, **139**, 12267–12273.

33 J. T. DuBose and P. V. Kamat, *J. Phys. Chem. Lett.*, 2019, **10**, 6074–6080.

34 A. De, S. Das and A. Samanta, *ACS Energy Lett.*, 2020, **5**, 2246–2252.

35 S. Akhil, V. G. V. Dutt and N. Mishra, *Nanoscale*, 2021, **13**, 13142–13151.

36 E. Yassitepe, Z. Yang, O. Voznyy, Y. Kim, G. Walters, J. A. Castañeda, P. Kanjanaboops, M. Yuan, X. Gong, F. Fan, J. Pan, S. Hoogland, R. Comin, O. M. Bakr, L. A. Padilha, A. F. Nogueira and Ed. H. Sargent, *Adv. Funct. Mater.*, 2016, **26**(47), 8757–8763.

37 J. De Roo, M. Ibáñez, P. Geiregat, G. Nedelcu, W. Walravens, J. Maes, J. C. Martins, I. Van Driessche, M. V. Kovalenko and Z. Hens, *ACS Nano*, 2016, **10**, 2071–2081.

38 P. M. Qureshi, R. K. Varshney and S. B. Singh, *Spectrochim. Acta, Part A*, 1994, **50**, 1789–1790.

39 K. E. Knowles, M. Tagliazucchi, M. Malicki, N. K. Swenson and E. A. Weiss, *J. Phys. Chem. C*, 2013, **117**, 15849–15857.

40 H. Lu, X. Zhu, C. Miller, J. San Martin, X. Chen, E. M. Miller, Y. Yan and M. C. Beard, *J. Chem. Phys.*, 2019, **151**, 204305.

